Development 136, 2535-2543 (2009) doi:10.1242/dev.033795

Sonic hedgehog signaling regulates a novel epithelial progenitor domain of the hindbrain choroid plexus

Xi Huang[1], Tatiana Ketova[1], Jonathan T. Fleming[1], Haibin Wang[2], Sudhansu K. Dey[3], Ying Litingtung[1] and Chin Chiang[1,*]

Choroid plexuses (ChPs) are vascularized secretory organs involved in the regulation of brain homeostasis, and function as the blood-cerebrospinal fluid (CSF) barrier. Despite their crucial roles, there is limited understanding of the regulatory mechanism driving ChP development. Sonic hedgehog (Shh), a secreted signal crucial for embryonic development and cancer, is strongly expressed in the differentiated hindbrain ChP epithelium (hChPe). However, we identify a distinct epithelial domain in the hChP that does not express Shh, but displays Shh signaling. We find that this distinct Shh target field that adjoins a germinal zone, the lower rhombic lip (LRL), functions as a progenitor domain by contributing directly to the hChPe. By conditional *Shh* mutant analysis, we show that Shh signaling regulates hChPe progenitor proliferation and hChPe expansion through late embryonic development, starting around E12.5. Whereas previous studies show that direct contribution to the hChPe by the LRL ceases around E14, our findings reveal a novel tissue-autonomous role for Shh production and signaling in driving the continual growth and expansion of the hindbrain choroid plexus throughout development.

KEY WORDS: Shh, Cerebrospinal fluid, Choroid plexus, Epithelium, Gli1

INTRODUCTION

Choroid plexuses (ChPs) are heavily vascularized secretory organs in the brain, which serve as sites of cerebrospinal fluid (CSF) production and are also known to generate chemicals and polypeptides with neuroprotective, surveillance and repair functions. The ChP epithelium has been the focus of extensive studies, as it serves as the blood-CSF barrier (Redzic et al., 2005; Segal, 2000). ChPs originate from four focal sites at the roof of the brain ventricles: two in the lateral ventricles of the telencephalon, one in the third ventricle of the diencephalon and one in the fourth ventricle of the hindbrain (hChP). Among all ChPs, hChP emerges earliest during embryogenesis and is conspicuously large. Outgrowth of the hChP is clearly evident at E12.5 as a pair of bilateral ridges protruding from the roof of the hindbrain, gradually developing into a highly convoluted organ with extensive epithelial folding. hChP consists of an outer epithelial layer and an inner core of stromal cells that are surrounded by a dense vascular network. The hChP epithelium (hChPe) initially emerges as a single sheet of pseudostratified cells, but by E13.5 the hChPe adopts a simple columnar morphology with numerous microvilli at the surface (Sturrock, 1979). Previous studies suggest that the rhombic lip, a germinal zone, first gives rise to the hindbrain roof plate epithelium (hRPe), which is further specified, potentially by high levels of Bmp signaling (Hebert et al., 2002), into definitive hChPe (Thomas and Dziadek, 1993). Genetic fate-mapping studies have shown that hChPe cells are derived from progenitor cells residing in the anterior lower rhombic lip (LRL), which is positioned between the developing hChP and medulla, with the expression of secreted growth factors Wnt1, Gdf7 and LIM-domain transcription factor Lmx1a (Awatramani et al., 2003; Chizhikov et al., 2006; Currle et al., 2005). A recent study indicates that Wnt1-expressing LRL cells can directly contribute to hChPe from E10 to E14 but this contribution ceases around E14 (Hunter and Dymecki, 2007). However, continued growth of the hChP beyond E14 suggests contribution by other hChPe progenitor sources besides early contribution by the hRPe and anterior LRL.

The *Shh* gene encodes a secreted signaling molecule that is indispensable for animal development. Patched 1 (Ptch1), a 12-pass transmembrane receptor for Shh, functions as a negative regulator of Shh signaling by suppressing the activity of a 7-pass transmembrane protein, Smoothened (Smo). Shh binding to Ptch1 relieves Smo from inhibition, hence triggering Shh signaling and subsequent activation of downstream target gene expression mediated by the Gli family of transcription factors (Ingham and McMahon, 2001). *Gli1* is the only member whose expression is directly regulated by Shh signaling at the transcriptional level and, like *Ptch1* expression, it serves as a direct readout of Shh pathway activation (Ahn and Joyner, 2004; Goodrich et al., 1996).

In the central nervous system (CNS), Shh is well recognized for its role in patterning different ventral neuronal cell types during early embryogenesis and in promoting cerebellar granule precursor cell proliferation (Goodrich et al., 1997; Wallace, 1999; Dahmane and Ruiz i Altaba, 1999; Wechsler-Reya and Scott, 1999). However, the role of Shh signaling during early embryonic CNS development is largely confined to the ventral regions. Interestingly, a recent study reported that Shh functions as an indispensable mitogen during dorsal telencephalic development (Komada et al., 2008). Nevertheless, a definitive dorsal role of Shh has not been generally appreciated. Here we have identified a distinct proliferating hChPe progenitor domain, adjoining the anterior LRL, displaying Shh signaling. Although direct contribution to the hChPe by cells of the LRL may have ceased by E14 (Hunter and Dymecki, 2007), our finding indicates that Shh signaling promotes proliferation of cells in the hChPe progenitor

[1]Department of Cell and Developmental Biology, Vanderbilt University Medical Center, 4114 MRB III, Nashville, TN 37232, USA. [2]State Key Laboratory of Reproductive Biology, Institute of Zoology, Chinese Academy of Sciences, Beijing 10010, China. [3]Division of Reproductive Sciences, Cincinnati Children's Research Foundation, 3333 Burnet Avenue, Cincinnati, OH 45229, USA.

*Author for correspondence (e-mail: chin.chiang@vanderbilt.edu)

Accepted 18 May 2009

domain, and thus contributes to the continual growth and expansion of the dorsally situated hChP throughout embryonic development.

MATERIALS AND METHODS

Mice

Wnt1-Cre (Jiang et al., 2000), *Gdf7-Cre* (Lee et al., 2000), *Shh*$^{fl/fl}$ (Lewis et al., 2001), *SmoM2* (Jeong et al., 2004), *Ptch1*$^{LacZ/+}$ (Goodrich et al., 1997), *Gli1-Cre*^{ERT2} (Ahn and Joyner, 2004), *ROSA26-LacZ* (Soriano, 1999) and *ROSA26-eYFP* (Srinivas et al., 2001) mice have been described previously.

Immunohistochemistry

All immunohistochemistry analyses were performed on tissue sections collected from OCT- or paraffin-embedded embryos as previously described (Huang et al., 2007). Primary antibodies were rabbit anti-Shh (Santa Cruz Biotechnology, 1:1000), rabbit anti-β-Gal (Cappel, 1:100), rabbit anti-aquaporin 1 (Chemicon, 1:500), rabbit anti-Lmx1a (gift of Dr Michael German, UCSF, San Francisco, CA, USA; 1:200), mouse anti-BrdU (Roche Diagnostics, 1:50), rabbit anti-GFP (Molecular Probes, 1:500) and rabbit anti-cleaved caspase 3 (Cell Signaling Technology, 1:100).

Analysis of cell proliferation and apoptosis

Bromodeoxyuridine (BrdU) in vivo labeling and terminal deoxynucleotidyl transferase mediated dUTP nick end labeling (TUNEL) analyses were performed as previously described (Huang et al., 2007).

Cell imaging, counting and statistics

Confocal microscopy was performed on immunofluorescent-stained sections with 1 μm optical slices. Independent stainings were performed on at least three animals for each marker and at least ten nonoverlapping sections were counted to generate statistical comparisons. For a 1-hour short-term BrdU pulse, Lmx1a^{+}; BrdU^{+} cells in the developing hChP region were located between the LRL and Aqp1-expressing differentiated hChPe. For quantifying proliferating hChPe progenitor cell numbers shown in Figs 3 and 6, and Fig. S4 in the supplementary material, the total number of Lmx1a^{+}; BrdU^{+} cells that spanned the putative hChPe progenitor domain adjoining the anterior LRL, identified by a characteristic bulge, was counted. For quantifying the number of BrdU^{+} cells after a 3-day pulse, contributing to the maturing hChPe shown in Fig. 4, the total numbers of BrdU^{+}; Aqp1^{+} hChPe cells, but not BrdU^{+}; Aqp1^{-} hChPm cells, were counted in randomly selected fields under 400× magnification. Only cells with purple-stained Aqp1^{+} membrane contacting a brown-stained BrdU^{+} nucleus were scored. To assess differences among groups, statistical analyses were performed using a one-way analysis of variance (ANOVA) with Microsoft Excel and significance accepted at $P<0.05$. Results are presented as mean±standard deviation (s.d.).

Tamoxifen treatment for temporal fate-mapping studies

Tamoxifen powder (Sigma T-5648) was dissolved in corn oil (Sigma C-8267) at a final concentration of 20 mg/ml. Pregnant females with E13 or E15 embryos from matings between *Gli1-Cre*^{ERT2} and *ROSA26-LacZ* or *ROSA26-eYFP* conditional and reporter mice, respectively, were each intraperitoneally injected with 4 mg tamoxifen. Females with E15 embryos were reinjected with 4 mg tamoxifen at E17. Embryos were then harvested and genotyped at E16 (injection at E13) and at newborn stage (P0) for injections at E15 and E17. *Gli1-Cre*^{ERT2}*; ROSA* embryos were processed for β-galactosidase activity or YFP staining, which was followed by confocal microscopy.

X-Gal staining and transcript detection

X-Gal staining for β-galactosidase was performed according to standard protocols. The following cDNAs were used as templates for synthesizing digoxigenin-labeled riboprobes: *Shh*, *Gli1*, *Ptch1*, *Ptch2*, *Gli3*, *Ttr*, *Bmp4*, *Msx1*, *Tgfb1*, *Tgfb3*, *spry1* and *spry2*.

RESULTS

Shh expression and signaling fields in the hindbrain choroid plexus

The hChP is generated bilaterally, protruding into the fourth ventricle, and is clearly evident at E12.5 (Fig. 1A,B). It undergoes dramatic growth and expansion as development progresses and joins at the midline (Fig. 1D-I). By E16.5, the hChP has developed into a highly convoluted epithelial structure enveloping a vascularized stroma (Fig. 1G,H). We observed strong *Shh* mRNA expression in the developing hChP epithelium (hChPe) starting at ~E12.5, and its expression persisted through to E18.5, the latest

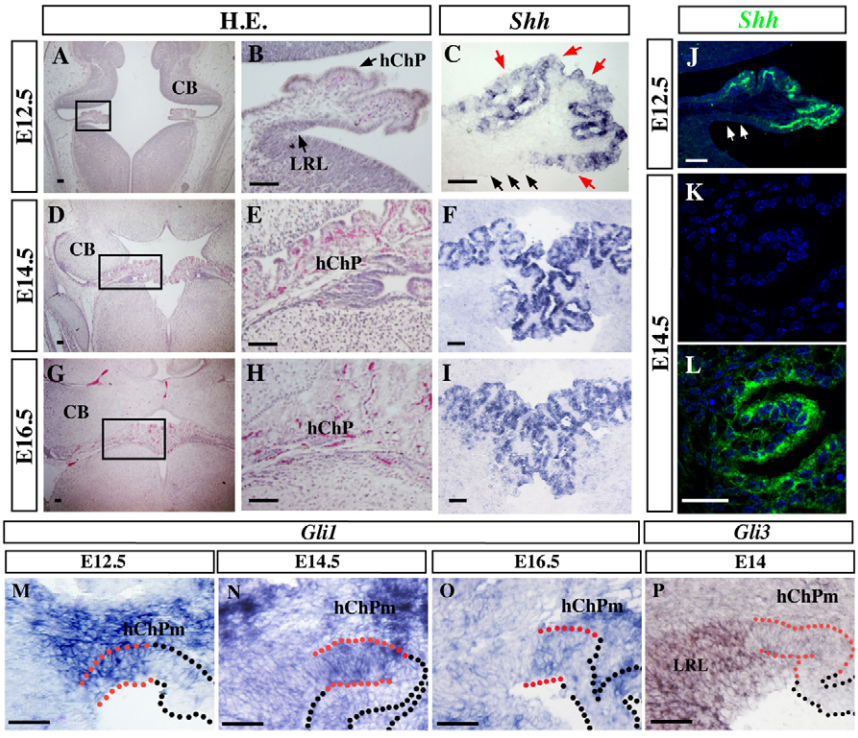

Fig. 1. Differentiated hChPe expresses Shh that signals to the underlying mesenchyme (hChPm) and to a distinct epithelial domain adjoining the lower rhombic lip (LRL). (**A-I**) Rapidly expanding hChPe expresses *Shh* in its differentiated epithelial domain. HE-stained images (A,B,D,E,G,H) and *Shh* in situ hybridization (C,F,I) at E12.5 (A-C), E14.5 (D-F) and E16.5 (G-I). Concomitant with hChP development and epithelial folding (A-I), hChPe cells strongly express *Shh* RNA (C,F,I). Note that *Shh* expression is either low or absent in a subset of hChPe cells, as indicated by red arrows in C. Black arrows in C point to the hChPe region adjoining the LRL that does not express *Shh* RNA. Boxes in A, D and G indicate magnified regions shown in B, E and H. (**J-L**) Shh protein (green) localizes to both apical and basolateral domains of hChPe cells at E12.5 (J) and E14.5 (K,L); nuclei are blue; J and L are merged images. Arrows in J indicate hChPe domain adjoining the LRL lacking Shh protein expression. (**M-O**) Shh signaling (indicated by *Gli1* expression) is robust in the developing hChPm, as well as in a distinct hChP epithelial domain adjoining the LRL indicated by red dotted lines (Gli1^{+}); black dotted lines are continuous with the rest of hChPe (Shh^{+} and Gli1^{-}). (M) E12.5, (N) E14.5, (O) E16.5. (**P**) *Gli3* is strongly expressed in the LRL, but not in the putative Gli1^{+} hChPe progenitor domain (red dotted line). Scale bars: 20 μm. CB, cerebellum; HE, hematoxylin and eosin.

stage analyzed (Fig. 1C,F,I; data not shown). In agreement, Shh protein is also highly expressed in the hChPe, with localization to both the apical and basolateral sides (Fig. 1J,K,L). Interestingly, a small subset of hChPe cells appeared to express low or no *Shh* transcript at various developmental stages (red arrows in Fig. 1C and Fig. S1 in the supplementary material). We detected strong Shh signaling in the underlying hChP mesenchyme (hChPm), as shown by the expression of Shh signaling targets *Gli1* and *Ptch1* (Fig. 1M,N,O; Fig. S1 in the supplementary material). Notably, we also identified a novel Shh target field within the developing hChP region, a restricted epithelial domain intercalated between the anterior LRL and the differentiated hChPe (Fig. 1; Fig. S1 in the supplementary material, red dotted lines). This Gli1^{+} hChPe domain does not express Shh (arrows in Fig. 1C,J; Fig. S1 in the supplementary material). By contrast, the differentiated hChPe expresses Shh but does not display apparent Shh signaling activity (Fig. 1; Fig. S1 in the supplementary material, black dotted lines). We did not detect *Ptch2* expression in the developing hChP, whereas its expression was readily detected in the hair follicles (see Fig. S2 in the supplementary material) (Motoyama et al., 1998). Interestingly, Gli3, a transcriptional repressor in the absence of Shh pathway activity, is expressed in the adjoining LRL but excluded from the putative hChPe progenitor domain (Fig. 1P). We barely detected *Gli1* signal in the telencephalic and diencephalic ChP regions at various developmental stages (data not shown), consistent with the fact that during embryogenesis only the hindbrain ChP expresses *Shh*, whereas the telencephalic and diencephalic ChPs do not (Tannahill et al., 2005) (data not shown).

Conditional abrogation of Shh signaling in *Wnt1-Cre; Shh$^{fl/-}$* mutants leads to impaired hChP development

To determine the functional role of Shh signaling during hChP development, we employed the Cre/*loxP* strategy to conditionally remove Shh in the hChPe. Previous genetic fate-mapping studies indicated that the hChP consists entirely of descendants of Wnt1-expressing cells that localize to the LRL (Hunter and Dymecki, 2007). Indeed, we detected β-galactosidase activity uniformly in the hChPe when the *Wnt1-Cre* driver line was crossed to the *ROSA26-LacZ* reporter strain (Fig. 2A,B). Therefore, the *Wnt1-Cre* driver line is suitable for deleting *Shh* in the hChPe. The effectiveness of *Wnt1-Cre* deletion of *Shh* was confirmed by essentially ablating *Shh* and *Gli1* expression in the *Wnt1-Cre*; *Shh$^{fl/-}$* mutant hChP region (compare Fig. 2C,D with Fig. 1C,M). Significant loss of Shh signaling in both the epithelial and mesenchymal target fields of the hChP resulted in severe defects in hChP development by E16.5. The *Wnt1-Cre*; *Shh$^{fl/-}$* mutant hChPs were hypoplastic with markedly reduced epithelial folding at E16.5 (compare Fig. 2E,F with 2G,H). The underdeveloped *Wnt1-Cre*; *Shh$^{fl/-}$* mutant hChPm also showed decreased vascularity (compare Fig. 2E,F with 2G,H). However, *Wnt1-Cre*; *Shh$^{fl/-}$* mutant hChPe maintained its molecular identity, as evidenced by the expression of the differentiated hChPe marker transthyretin (*Ttr*) and water channel aquaporin 1 (Aqp1), expressed apically (Fig. 2I-L). Furthermore, abrogating Shh signaling in the hChP did not appear to alter its ability to produce other growth factors, such as *Bmp4* and *Tgfb3* in the hChPe or *Tgfb1* in the hChPm (Fig. 2M-P; data not shown). The Fgf signaling pathway does not appear to regulate

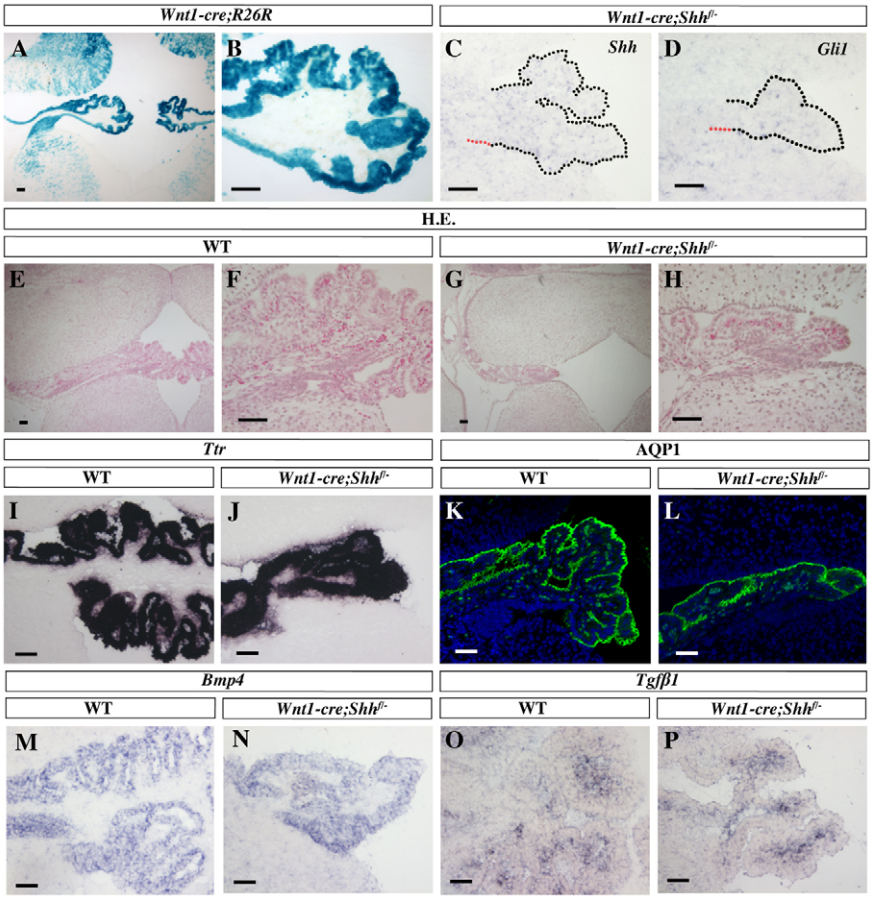

Fig. 2. Genetic removal of Shh signaling impairs hChP biogenesis. (**A-D**) The transgenic *Wnt1-Cre* line effectively drives gene deletion in hChPe cells, as indicated by a strong β-Gal staining signal in E13.5 *Wnt1-Cre; R26R* embryos (A,B) and abrogated *Shh* expression (C) and signaling (*Gli1* expression, D) in E14.5 *Wnt1-Cre*; *Shh$^{fl/-}$* mutant hChP. (**E-H**) E16.5 *Wnt1-Cre*; *Shh$^{fl/-}$* mutants (G,H) display severely affected hChP development as indicated by an apparent reduction in epithelial and mesenchymal mass and vascularity compared with wild type (E,F). (**I-P**) hChPe cell differentiation and ability to produce other signaling factors appear to be unaffected by loss of Shh signaling. E14.5 *Wnt1-Cre*; *Shh$^{fl/-}$* mutant hChPe cells (J,L,N,P) maintain expression of the differentiation marker *Ttr* (I,J), the apical marker Aqp1 (K,L), and signaling molecules *Bmp4* (M,N) and *Tgfb1* (O,P). Scale bars: 20 μm.

hChP development directly, as we did not detect appreciable expression of sprouty 1 and 2, which are target genes of the Fgf signaling pathway (Minowada et al., 1999) (see Fig. S2 in the supplementary material). These findings indicate that the growth defects seen in *Wnt1-Cre*; *Shh*$^{fl/-}$ mutant hChP are primarily due to the inability to perceive Shh signaling. Therefore, Shh production in the differentiated hChPe domain and Shh signaling within the hChP, including the distinct epithelial domain adjoining the LRL, are crucial for hChP development.

Shh signaling promotes proliferation of a distinct hChP epithelial progenitor domain

Next, in order to elucidate the molecular mechanism of hChPe growth during development, we focused on determining the function of Shh signaling in the hChP epithelial target field. As mentioned above, whereas the Gli1^{-} differentiated hChPe expressing Aqp1 did not appear to display Shh signaling (Fig. 1; Fig. 3A,B, black dotted lines), we observed distinct Shh signaling (Gli1^{+}) in a restricted epithelial domain adjoining the anterior edge of the LRL extending towards the hChPe (Fig. 1M,N,O; see Fig. S1 in the supplementary material; Fig. 3A,B, red dotted lines). As we observed a marked reduction in hChP growth in *Wnt1-Cre*; *Shh*$^{fl/-}$ mutants, we asked whether this Gli1^{+} hChPe region defined an hChPe progenitor domain, and we used Lmx1a expression to mark all cells in the hChPe (Chizhikov et al., 2006). Indeed, in *Ptch1*$^{LacZ/+}$ embryos the β-Gal^{+} Shh signaling domain overlapped with the Lmx1a-expressing domain adjoining the LRL (Fig. 3C-I, white arrows in E,F; G-I correspond to the red boxed region shown in C), indicating that Shh signaling occurred in this crucial domain. We determined that this specific Lmx1a^{+} hChPe domain also displayed proliferative activity, as indicated by its rapid incorporation of BrdU and expression of Ki67 (Mki67 – Mouse Genome Informatics) (Fig. 3J-M; data not shown). By contrast, the rest of the hChPe was *Ptch1*$^{-}$ and *Gli1*$^{-}$ (Fig. 1M-O; Fig. 3A,B; Fig. S1 in the supplementary material, black dotted lines) and postmitotic, as these cells did not show BrdU incorporation (after a 1-hour short-term pulse) or Ki67 expression (Fig. 3J-M; data not shown). Therefore, we propose that Shh pathway activity in the proliferating domain is a distinct hChPe domain harboring progenitor cells, which gives rise to nascent differentiated hChPe as development progresses. In agreement, we observed more than a 2-fold reduction in proliferating cells in this hChPe progenitor region in *Wnt1-Cre*; *Shh*$^{fl/-}$ mutants compared

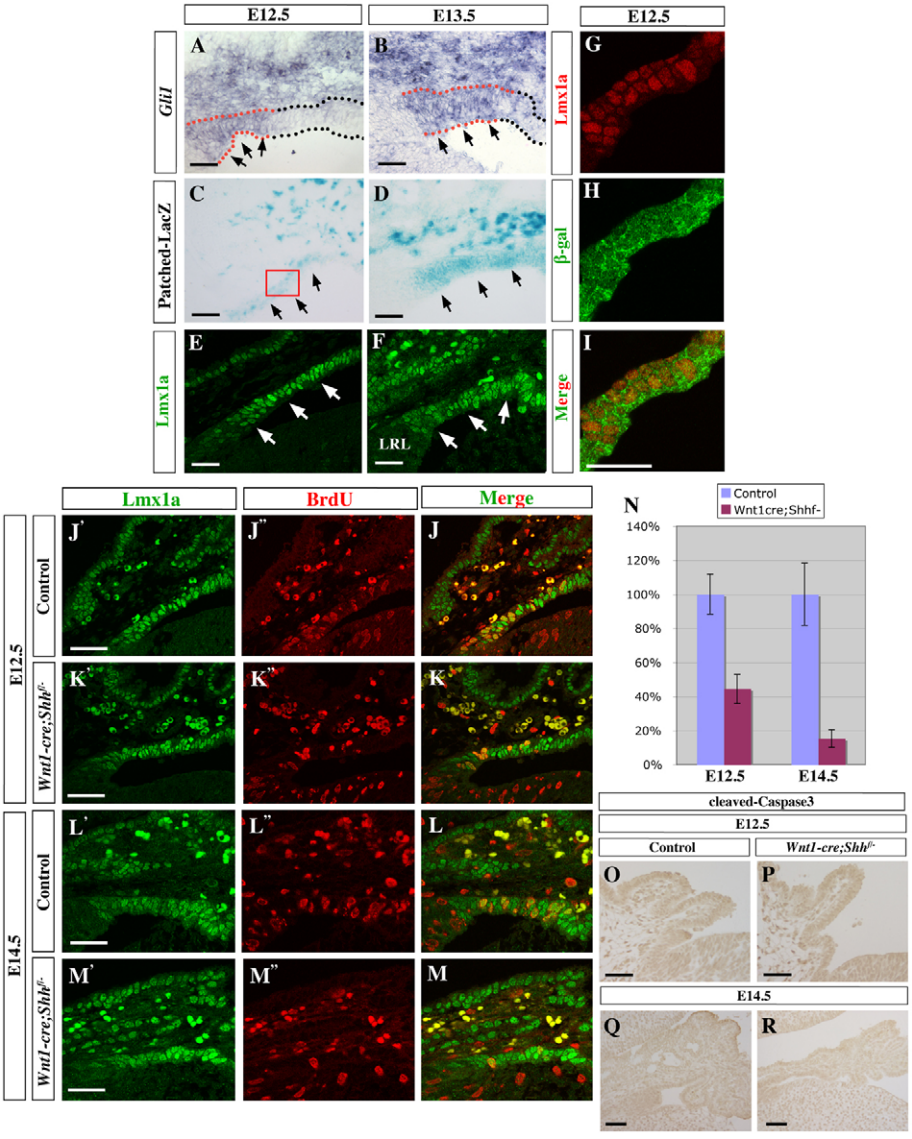

Fig. 3. Shh signaling defines an Lmx1a^{+} hChPe progenitor domain and promotes its proliferation. (**A-I**) Shh signals to a distinct Lmx1a^{+} domain adjoining the anterior LRL. Shh signaling activity, as evidenced by *Gli1* (A,B) and *Ptch1-LacZ* (C,D) expression, overlaps with this distinct Lmx1a^{+} domain (compare A-D with E,F), which is confirmed by the colabeling of Lmx1a and β-Gal activity in *Ptch1*$^{LacZ/+}$ embryos (G-I). The hChPe progenitor domain adjoining the LRL is highlighted by red dotted lines and arrows in A and B. Black dotted lines demarcate the rest of the hChPe (Gli1^{-}). Arrows in C-F indicate the putative hChPe progenitor domain. (**J-N**) Genetic deletion of Shh signaling results in severe proliferation defects in the progenitor domain. Colabeling of BrdU (red, J″-M″) and Lmx1a (green, J′-M′) in 1-hour BrdU-pulsed control and *Wnt1-Cre*; *Shh*$^{fl/-}$ embryos reveals a profound proliferation defect at E12.5 (J-K″,N) and E14.5 (L-M″,N). The proliferation defect is even more severe at E14.5 (N). (**O-R**) Loss of Shh signaling does not appear to affect cell survival in the hChP, as indicated by the absence of cleaved-caspase 3 activity in E12.5 (O,P) or E14.5 (Q,R) control and *Wnt1-Cre*; *Shh*$^{fl/-}$ embryos. Scale bars: 20 μm.

with controls at E12.5 (44.4±8.5% versus 100±11.7%, P<0.001, n=3; Fig. 3J,K,N), and a more pronounced decline in BrdU$^+$ cells (~7-fold) at E14.5 (15.3±5.2% versus 100±18.3%, P<0.001, n=3; Fig. 3L,M,N).

We have also generated conditional *Gdf7*$^{Cre/+}$; *Shh*$^{fl/-}$ mutants using mice with *Cre* expression driven by the endogenous *Gdf7* promoter, which is expressed in all of the ChPe (Currle et al., 2005). However, we found that the knock-in *Gdf7*$^{Cre/+}$ line (Lee et al., 2000) is not as robust as the transgenic *Wnt1-Cre* line (Jiang et al., 2000) in driving complete Shh deletion in the hChPe (see Fig. S4 in the supplementary material). In agreement, we observed a relatively milder, but significant, hChP phenotype in *Gdf7*$^{Cre/+}$; *Shh*$^{fl/-}$ compared with *Wnt1-Cre*; *Shh*$^{fl/-}$ mutants at E14.5 (compare Fig. S4 in the supplementary material with Fig. 3). The finding that *Gdf7*$^{Cre/+}$; *Shh*$^{fl/-}$ mutants exhibited impaired proliferation in the Lmx1a$^+$ hChPe progenitor domain is consistent with our *Wnt1-Cre*; *Shh*$^{fl/-}$ mutant studies, lending further support for the essential role of Shh signaling in regulating hChPe progenitor proliferation. Shh signaling did not appear to be required for maintaining cell survival in the hChPe progenitor region, as neither controls nor *Wnt1-Cre*; *Shh*$^{fl/-}$ mutants displayed apparent apoptotic activity, as shown by TUNEL assay (data not shown) or cleaved-caspase 3 immunolabeling (Fig. 3O-R), even though apoptotic signals in the same sections were detected in peripheral nerve or muscle tissues between the developing ribs (see Fig. S3 in the supplementary material). Previous studies have shown direct LRL cell contribution to the hChPe but production appears to cease around E14. Here, we reveal the essential role of Shh signaling in promoting the proliferation of a distinct pool of hChPe progenitor cells in a domain adjoining the LRL, starting at ~E12.5 through late embryonic development, for the continual expansion of the hChP.

Shh signaling promotes proliferation of hChPe progenitor cells and hChPe biogenesis

To further define the role of Shh signaling in the production of hChPe cells, we performed BrdU pulse-chase labeling, for short and long periods, to compare the temporal contribution of nascent epithelial cells to the hChPe. By colabeling 1-hour-pulsed BrdU with the differentiated hChPe apical marker Aqp1, we observed a BrdU$^-$ Aqp1$^-$ region between the hChPe progenitor and differentiated hChPe domains (Fig. 4A,A′). Ki67 and Aqp1 double labeling demonstrated that this ‘gap’ region is nonmitotic (Fig. 4C,D). After a 24-hour pulse, the BrdU$^+$ cells had migrated to the region just adjoining the Aqp1$^+$ domain (Fig. 4B,B′, white arrow), suggesting a rather slow rate of progenitor contribution to the hChPe. However, after a 3-day BrdU pulse, starting at E13.5 or 14.5, we observed an extensive contribution of nascent BrdU$^+$ cells well into the differentiated hChPe (Fig. 4E,G,I). The BrdU$^+$ cell contribution to the hChPe in *Wnt1-Cre*; *Shh*$^{fl/-}$ mutants was evidently decreased by ~5-fold compared with controls upon analysis at E16.5 (22.1±4.8% versus 100±20.5%, P<0.001, n=3) (Fig. 4E-H,K) and E17.5 (24.6±7.5% versus 100±15.2%, P<0.001, n=3) (Fig. 4I-K). These results clearly indicate that hChPe progenitor proliferation in mutants had been compromised in the absence of Shh signaling.

To follow the fate of Gli1$^+$ cells in the hChPe progenitor domain, we performed tamoxifen injections on pregnant females from matings between *Gli1-Cre*^{ERT2} and *ROSA-LacZ* or *ROSA-eYFP* reporter mice at E13, or E15 and E17, respectively, and harvested embryos at E16 or P0. These temporal fate-mapping studies demonstrated that, indeed, cells derived from the Gli1$^+$ hChPe progenitor domain are incorporated into the mature hChPe (Fig. 5A-D, arrows). The later-stage tamoxifen injection appeared to label fewer cells in the hChPe, consistent with our finding that the

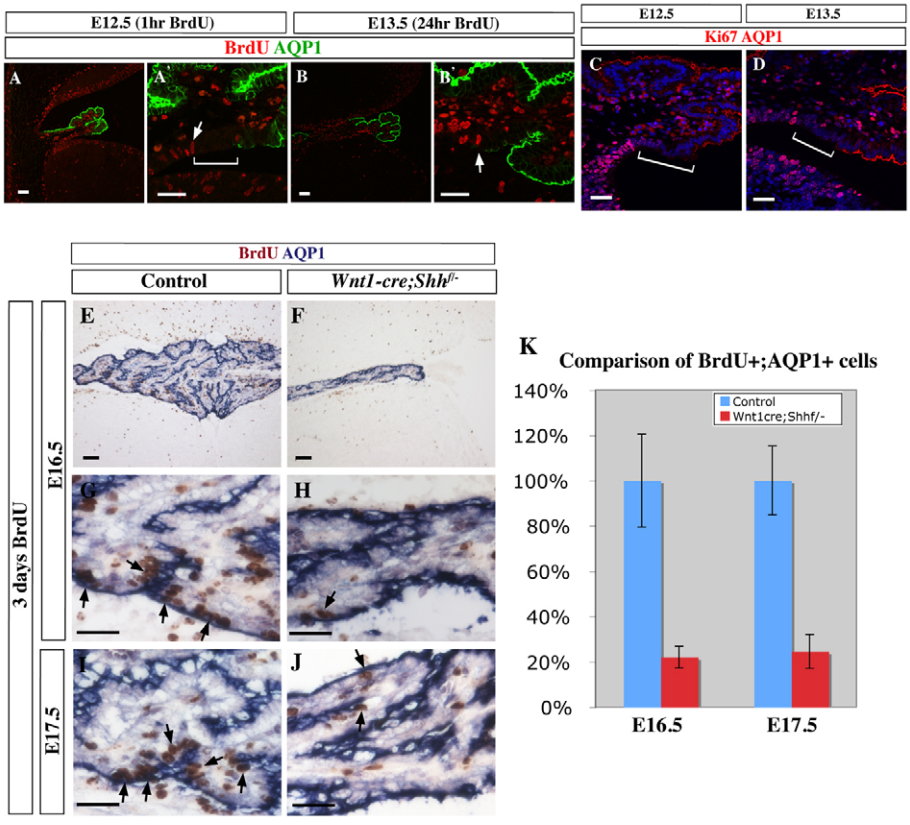

Fig. 4. Loss of Shh signaling leads to reduced hChPe production. (**A-D**) Nascent hChPe cells from the progenitor domain appear to be incorporated at a slow rate into the differentiated hChPe region (Aqp1$^+$). (A,A′) BrdU pulse labeling for 1 hour reveals a BrdU$^-$ and Aqp1$^-$ ‘gap’ region (bracket in A′,C,D) intercalated between the hChPe progenitor and differentiated domains; this gap region is nonmitotic, as indicated by the lack of Ki67 expression (C,D). (B,B′) Cells labeled after 24-hour BrdU pulse labeling now abut the Aqp1$^+$ hChPe domain (indicated by white arrow), indicating a rather slow process by which nascent hChPe cells become incorporated into the differentiated zone. (**E-K**) Loss of Shh signaling results in a largely reduced hChPe cell production in *Wnt1-Cre*; *Shh*$^{fl/-}$ mutants (F,H,J) compared with wild type (E,G,I). Black arrows indicate 3-day-pulsed BrdU$^+$ cells in the differentiated hChPe domain highlighted by Aqp1. Scale bars: 20 μm.

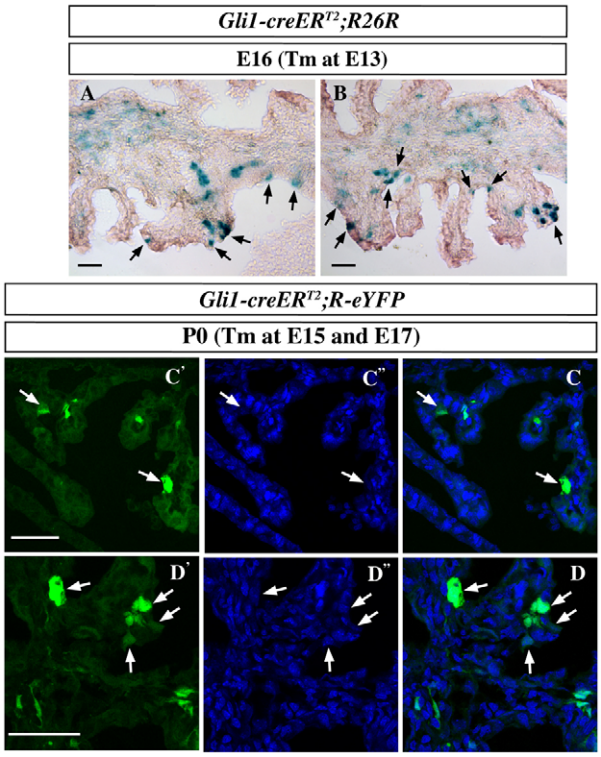

Fig. 5. Gli1$^+$ cells from the hChPe progenitor domain contribute to hChPe growth. Temporal fate-mapping of Gli1$^+$ Shh-responding cells in E16 (A,B) and P0 (C-D) hChPe domains with tamoxifen (Tm) injections at E13 (**A**,**B**), or at E15 and E17 (**C-D**). (A,B) X-Gal staining. (C-D) YFP staining in green (C′,D′), nuclear labeling in blue (C″,D″) and merged images (C,D). Black arrows in A, B and white arrows in C, D point to Gli1-marked hChPe cells. Cells of the Gli1$^+$ lineage are also evident in the hChPm. A and B show different representative X-gal-stained sections; C and D show two different representative YFP-stained sections. Scale bars: 20 μm.

Lmx1a$^+$ hChPe progenitor domain displayed reduced proliferative activity at late developmental and postnatal stages (Fig. 6; data not shown). We observed extensive *Gli1-Cre* activated gene recombination in the cerebellar external granule layer in the same embryo, indicating the efficacy of tamoxifen treatment (see Fig. S5 in the supplementary material). As tamoxifen usually begins to be effective in driving gene recombination ~12-24 hours postinjection, our data reveal that *Gli1*-expressing cells between ~E14 and E18 within the hChPe progenitor domain continue to be incorporated into the expanding hChPe. Taken together, these data demonstrate that Shh signaling is required to maintain a pool of proliferating cells in the hChPe progenitor domain and that these Gli1$^+$ cells appear to contribute to hChPe expansion beginning at ~E12.5 through to late developmental stages.

To further support the crucial proliferative role of Shh signaling during hChPe development, we generated *Wnt1-Cre; SmoM2* and *Gdf7$^{Cre/+}$; SmoM2* mutants, in which constitutively active SmoM2 (Jeong et al., 2004) is expressed in all hChPe cells. As *Wnt1-Cre* is also expressed in the neural crest lineage and widespread Shh pathway overactivation led to profound craniofacial and neural tube defects, including excencephaly, all subsequent analyses were performed using the *Gdf7$^{Cre/+}$* driver line. Interestingly, although ectopic Notch signaling has been reported to elicit persistent proliferation in many mature hChPe cells (Dang et al., 2006; Hunter and Dymecki, 2007), we observed enhanced mitotic activity that appeared to be confined to the putative hChPe progenitor region adjoining the anterior LRL in *Gdf7$^{Cre/+}$; SmoM2* mutants at E14.5 and at birth (Fig. 6). After a 1-hour pulse, we did not observe BrdU$^+$ cells within the Aqp1-expressing differentiated hChPe in either controls or *Gdf7$^{Cre/+}$; SmoM2* mutants (Fig. 6F,G). This observation suggests distinct regulatory mechanisms by which the Notch and Shh pathways expand the hChPe cell population. Although the number of proliferating Lmx1a$^+$ hChPe progenitor cells appeared to dwindle at birth (Fig. 6C,D), we observed enhanced proliferative activity in the hChPe progenitor domain in *Gdf7$^{Cre/+}$*; *SmoM2* mutants compared with controls at E14.5 (188.8±21.1% versus 100±10.9%, $P<0.001$, $n=3$) (Fig. 6A-B″,E) and P0 (161.2±25.9% versus 100±25.4%, $P<0.001$, $n=3$) (Fig. 6C-E). These gain-of-function studies further support our finding that Shh signaling is both necessary and sufficient to drive proliferation of hChPe progenitor cells.

Most *Gdf7$^{Cre/+}$*; *SmoM2* mutants do not survive beyond 3 weeks after birth. All mutants were runted and exhibited neurological defects reflected by their relative immobility compared with control littermates. Consistent with enhanced proliferation at the progenitor domain, the hChPs of *Gdf7$^{Cre/+}$*; *SmoM2* mutants appeared larger in size, displaying more epithelial foldings (Fig. 7). ChPs of the diencephalon and telencephalon might also be affected by expression of SmoM2, as the Gdf7 lineage maps to these choroid plexus epithelia. Therefore, the severe phenotype of *Gdf7$^{Cre/+}$*; *SmoM2* mutant neonates might be due to the combined aberrant function of ChPs and disruption in CNS homeostasis.

DISCUSSION

ChPs are secretory organs in the brain; they serve as sites of CSF production and function as blood-CSF barriers to maintain CNS homeostasis. Although Bmp signaling in the dorsal midline has been implicated in the specification of ChP epithelial fate (Cheng et al., 2006; Hebert et al., 2002), signaling mechanisms that regulate ChP epithelium production and expansion remain poorly understood. It has been reported that the hChP expresses many morphogens, such as Bmps, Fgfs, Tgfβs and Shh (Bitgood and McMahon, 1995; Emerich et al., 2005; Redzic et al., 2005). However, surprisingly little is known about the developmental mechanism or molecular pathway that regulates hChP biogenesis. Interestingly, choroid plexus tumor is a pediatric neoplasm characterized by uncontrolled growth of the ChP epithelium, and 40% of ChP tumors arise in the hindbrain ventricle (Gopal et al., 2008). Considering that Shh expression in the CNS is restricted to the ventral axial midline of the floor plate and the neuroectoderm before/at mid-gestation, it is quite unique that a dorsal roof-plate-derived hChP exhibits robust Shh expression. Here we show that Shh signaling plays an essential role in regulating hChPe progenitor cell proliferation and, thus, expansion of the hChP throughout embryogenesis (Fig. 8).

The hChP exhibits complex epithelial folding during development that vastly enlarges its surface area necessary for secretory functions. Therefore, it is essential to ensure adequate production of epithelial cells throughout hChP development. Previously, Bmp signaling has been found to specify the primitive pseudostratified epithelial domain into a definitive ChPe fate, demonstrated by the specific loss of ChP after telencephalic inactivation of the Bmp receptor Bmpr1a (Hebert et al., 2002).

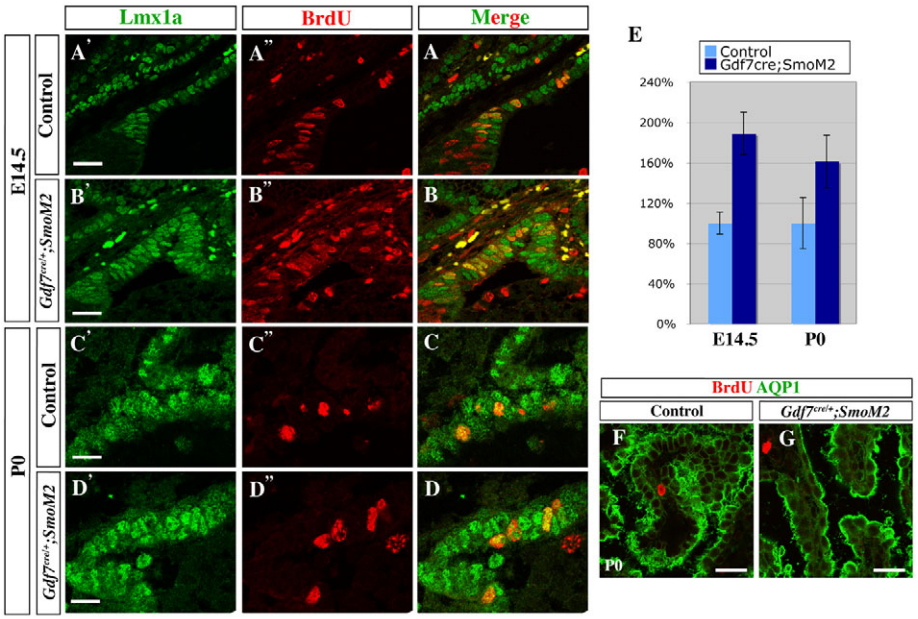

Fig. 6. Ectopic Shh signaling drives excessive Lmx1a^{+} hChPe progenitor cell proliferation. (**A-E**) *Gdf7$^{Cre/+}$; SmoM2* gain-of-function mutants display augmented proliferative activity in the Lmx1a^{+} hChPe progenitor domain at E14.5 (A-B,E) and P0 (C-D,E), further supporting a proliferative role of Shh signaling during hChPe production. (**F**,**G**) Ectopic Shh signaling did not render the differentiated Aqp1^{+} hChPe cells mitotic, as evidenced by a lack of BrdU signal after a 1-hour pulse. BrdU^{+} cells are present within the mesenchymal compartment of both controls (F) and *Gdf7$^{Cre/+}$; SmoM2* mutants (G). Scale bars: 20 μm.

Genetic fate-mapping studies suggested that the hChPe progenitor resides in the anterior LRL domain expressing Gdf7 and Lmx1a. The Notch signaling pathway has been shown to promote hChPe proliferation, as retrovirus-driven expression of the ligand Notch3 (Dang et al., 2006) and *Gdf7^{Cre}*-driven ectopic expression of the activated ligand Notch1^{ICD} (Hunter and Dymecki, 2007) both led to the persistent proliferation of hChPe cells. Conversely, global inactivation of Notch signaling in zebrafish resulted in defective ChP development (Bill et al., 2008; Garcia-Lecea et al., 2008). However, these overexpression and global gene inactivation analyses yielded limited information on whether Notch signaling regulates the proliferative capacity of hChPe progenitor domain in a physiologically unperturbed situation, and what cell population Notch signaling directly targets. Indeed, we observed that Notch1

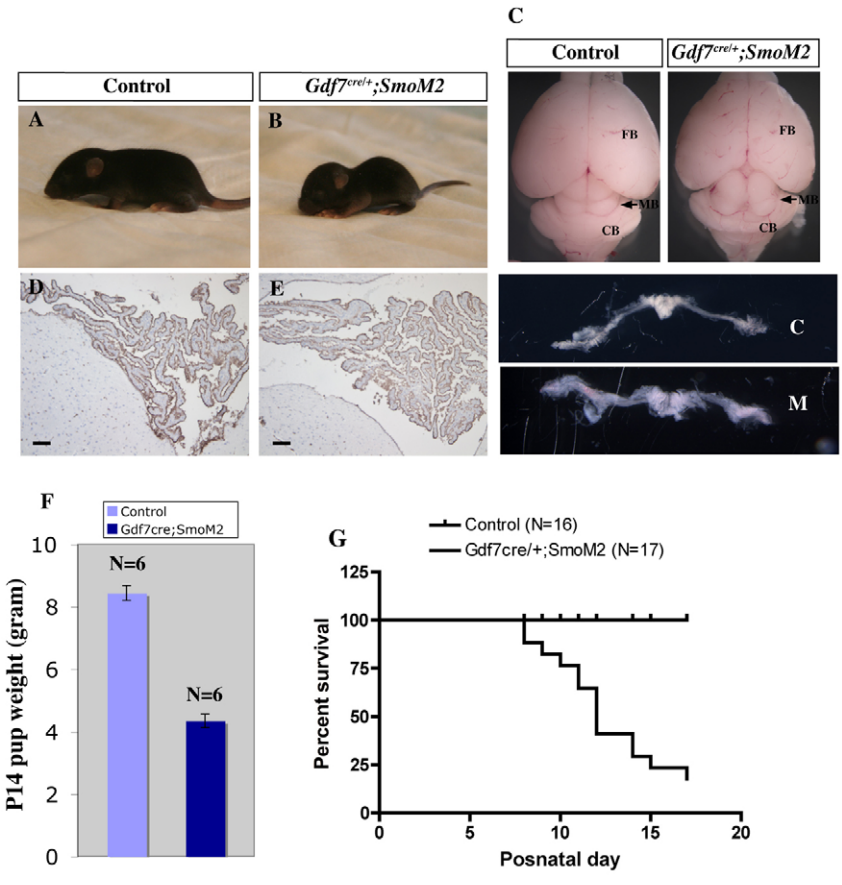

Fig. 7. Postnatal studies of gain-of-function *Gdf7$^{Cre/+}$; SmoM2* mutants. (**A**,**B**) External view of postnatal day 10 control (A) and *Gdf7$^{Cre/+}$; SmoM2* mutant (B) pups. The *Gdf7$^{Cre/+}$; SmoM2* mutant shows severely stunted growth and is relatively immobile. (**C**) *Gdf7$^{Cre/+}$; SmoM2* mutant and control brains appear comparable in size, yet the wholly dissected hChP of the mutant (M, bottom panel) appears enlarged relative to the control (C, middle panel). (**D**,**E**) Despite the much smaller body size of *Gdf7$^{Cre/+}$; SmoM2* mutants, their hChPs appear to be larger, displaying more epithelial folds than controls. (**F**) *Gdf7$^{Cre/+}$; SmoM2* mutants are significantly smaller than controls. (**G**) Most *Gdf7$^{Cre/+}$; SmoM2* mutants do not survive beyond 3 weeks after birth. Scale bar: 20 μm. CB, cerebellum; FB, forebrain; MB, midbrain.

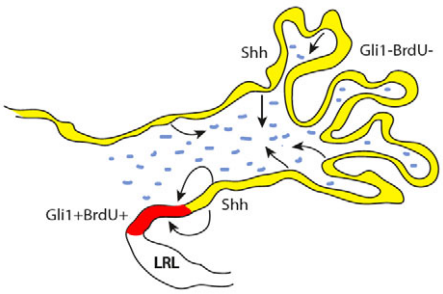

Fig. 8. Compartmentalization of Shh expression and signaling in the hChP. *Shh* expression in the differentiated hChPe (yellow, Gli1$^-$ BrdU$^-$) activates Shh signaling in two hChP target fields: the hChPe progenitor domain (red, Gli1$^+$ BrdU$^+$) and the mesenchyme (blue). Since Shh protein is distributed in both the apical and basal membranes of the differentiated hChPe, Shh movement to the hChPe progenitor domain could potentially occur via either or both routes (curved arrows). LRL, lower rhombic lip.

expression encompasses the entire LRL (X.H. and C.C., unpublished), indicative of a broader function of Notch signaling rather than Notch specifically acting on expanding the hChPe progenitor domain.

Here, our study identifies a Shh signaling hChPe progenitor domain adjoining the anterior LRL. Loss- and gain-of-function analyses demonstrated that Shh signaling functions specifically to promote proliferation of this hChPe progenitor domain to ensure sufficient production of nascent hChPe cells that gradually get incorporated into the medial differentiated hChPe. Therefore, we propose that Shh signaling defines a novel Lmx1a$^+$ hChPe progenitor domain, and Shh pathway activation is essential for regulating the proliferation of these progenitor cells, which is crucial for hChP biogenesis from ~E12.5 through to late stages of development.

The finding that Shh signaling promotes the proliferation of epithelial progenitor cells destined to become part of the hChPe, which is itself a primary source of the Shh ligand, reveals an interesting biological phenomenon in which the Shh target and producing cells are part of the same tissue, the ependymal epithelium. We show that Shh produced in the hChPe not only signals to the mesenchyme, a classic example of an epithelial-mesenchymal interaction, but also to its own progenitor domain, and is thus a unique example of two distinct target fields within one organ (Fig. 8). In several endoderm-derived organs displaying epithelial-mesenchymal interactions, it is thought that Shh produced by the epithelium exclusively signals to the mesenchyme, which in turn generates another mitogenic signal to promote epithelial proliferation. Although the hChP mesenchyme could also contribute to hChPe growth, our finding reveals a tissue-autonomous role of hChPe with regard to Shh production and signaling in driving the growth and expansion of a conspicuously large hindbrain choroid plexus.

Acknowledgements

We are grateful to Tom Jessell, Jane Dodd and Alex Joyner for providing *Gdf7-Cre* and *Gli1-Cre^{ERT2}* mice; Michael German for generously providing the Lmx1a antibody; and Sean Schaffer at the Vanderbilt University Cell Imaging Shared Resource for his help with confocal microscopy (supported by grant CA068485). This study was supported by a grant from the National Institutes of Health (grant number NS042205). Deposited in PMC for release after 12 months.

Supplementary material

Supplementary material for this article is available at http://dev.biologists.org/cgi/content/full/136/15/2535/DC1

References

Ahn, S. and Joyner, A. L. (2004). Dynamic changes in the response of cells to positive hedgehog signaling during mouse limb patterning. *Cell* **118**, 505-516.

Awatramani, R., Soriano, P., Rodriguez, C., Mai, J. J. and Dymecki, S. M. (2003). Cryptic boundaries in roof plate and choroid plexus identified by intersectional gene activation. *Nat. Genet.* **35**, 70-75.

Bill, B. R., Balciunas, D., McCarra, J. A., Young, E. D., Xiong, T., Spahn, A. M., Garcia-Lecea, M., Korzh, V., Ekker, S. C. and Schimmenti, L. A. (2008). Development and Notch signaling requirements of the zebrafish choroid plexus. *PLoS ONE* **3**, e3114.

Bitgood, M. J. and McMahon, A. P. (1995). Hedgehog and Bmp genes are coexpressed at many diverse sites of cell-cell interaction in the mouse embryo. *Dev. Biol.* **172**, 126-138.

Cheng, X., Hsu, C. M., Currle, D. S., Hu, J. S., Barkovich, A. J. and Monuki, E. S. (2006). Central roles of the roof plate in telencephalic development and holoprosencephaly. *J. Neurosci.* **26**, 7640-7649.

Chizhikov, V. V., Lindgren, A. G., Currle, D. S., Rose, M. F., Monuki, E. S. and Millen, K. J. (2006). The roof plate regulates cerebellar cell-type specification and proliferation. *Development* **133**, 2793-2804.

Currle, D. S., Cheng, X., Hsu, C. M. and Monuki, E. S. (2005). Direct and indirect roles of CNS dorsal midline cells in choroid plexus epithelia formation. *Development* **132**, 3549-3559.

Dahmane, N. and Ruiz i Altaba, A. (1999). Sonic hedgehog regulates the growth and patterning of the cerebellum. *Development* **126**, 3089-3100.

Dang, L., Fan, X., Chaudhry, A., Wang, M., Gaiano, N. and Eberhart, C. G. (2006). Notch3 signaling initiates choroid plexus tumor formation. *Oncogene* **25**, 487-491.

Emerich, D. F., Skinner, S. J., Borlongan, C. V., Vasconcellos, A. V. and Thanos, C. G. (2005). The choroid plexus in the rise, fall and repair of the brain. *BioEssays* **27**, 262-274.

Garcia-Lecea, M., Kondrychyn, I., Fong, S. H., Ye, Z. R. and Korzh, V. (2008). In vivo analysis of choroid plexus morphogenesis in zebrafish. *PLoS ONE* **3**, e3090.

Goodrich, L. V., Johnson, R. L., Milenkovic, L., McMahon, J. A. and Scott, M. P. (1996). Conservation of the hedgehog/patched signaling pathway from flies to mice: induction of a mouse patched gene by Hedgehog. *Genes Dev.* **10**, 301-312.

Goodrich, L. V., Milenkovic, L., Higgins, K. M. and Scott, M. P. (1997). Altered neural cell fates and medulloblastoma in mouse patched mutants. *Science* **277**, 1109-1113.

Gopal, P., Parker, J. R., Debski, R. and Parker, J. C., Jr (2008). Choroid plexus carcinoma. *Arch. Pathol. Lab. Med.* **132**, 1350-1354.

Hebert, J. M., Mishina, Y. and McConnell, S. K. (2002). BMP signaling is required locally to pattern the dorsal telencephalic midline. *Neuron* **35**, 1029-1041.

Huang, X., Litingtung, Y. and Chiang, C. (2007). Ectopic sonic hedgehog signaling impairs telencephalic dorsal midline development: implication for human holoprosencephaly. *Hum. Mol. Genet.* **16**, 1454-1468.

Hunter, N. L. and Dymecki, S. M. (2007). Molecularly and temporally separable lineages form the hindbrain roof plate and contribute differentially to the choroid plexus. *Development* **134**, 3449-3460.

Ingham, P. W. and McMahon, A. P. (2001). Hedgehog signaling in animal development: paradigms and principles. *Genes Dev.* **15**, 3059-3087.

Jeong, J., Mao, J., Tenzen, T., Kottmann, A. H. and McMahon, A. P. (2004). Hedgehog signaling in the neural crest cells regulates the patterning and growth of facial primordia. *Genes Dev.* **18**, 937-951.

Jiang, X., Rowitch, D. H., Soriano, P., McMahon, A. P. and Sucov, H. M. (2000). Fate of the mammalian cardiac neural crest. *Development* **127**, 1607-1616.

Komada, M., Saitsu, H., Kinboshi, M., Miura, T., Shiota, K. and Ishibashi, M. (2008). Hedgehog signaling is involved in development of the neocortex. *Development* **135**, 2717-2727.

Lee, K. J., Dietrich, P. and Jessell, T. M. (2000). Genetic ablation reveals that the roof plate is essential for dorsal interneuron specification. *Nature* **403**, 734-740.

Lewis, P. M., Dunn, M. P., McMahon, J. A., Logan, M., Martin, J. F., St-Jacques, B. and McMahon, A. P. (2001). Cholesterol modification of sonic hedgehog is required for long-range signaling activity and effective modulation of signaling by Ptc1. *Cell* **105**, 599-612.

Minowada, G., Jarvis, L. A., Chi, C. L., Neubuser, A., Sun, X., Hacohen, N., Krasnow, M. A. and Martin, G. R. (1999). Vertebrate Sprouty genes are induced by FGF signaling and can cause chondrodysplasia when overexpressed. *Development* **126**, 4465-4475.

Motoyama, J., Takabatake, T., Takeshima, K. and Hui, C. (1998). Ptch2, a second mouse Patched gene is co-expressed with Sonic hedgehog. *Nat. Genet.* **18**, 104-106.

Redzic, Z. B., Preston, J. E., Duncan, J. A., Chodobski, A. and Szmydynger-Chodobska, J. (2005). The choroid plexus-cerebrospinal fluid system: from development to aging. *Curr. Top. Dev. Biol.* **71**, 1-52.

Segal, M. B. (2000). The choroid plexuses and the barriers between the blood and the cerebrospinal fluid. *Cell. Mol. Neurobiol.* **20**, 183-196.
Soriano, P. (1999). Generalized lacZ expression with the ROSA26 Cre reporter strain. *Nat. Genet.* **21**, 70-71.
Srinivas, S., Watanabe, T., Lin, C. S., William, C. M., Tanabe, Y., Jessell, T. M. and Costantini, F. (2001). Cre reporter strains produced by targeted insertion of EYFP and ECFP into the ROSA26 locus. *BMC Dev. Biol.* **1**, 4.
Sturrock, R. R. (1979). A morphological study of the development of the mouse choroid plexus. *J. Anat.* **129**, 777-793.
Tannahill, D., Harris, L. W. and Keynes, R. (2005). Role of morphogens in brain growth. *J. Neurobiol.* **64**, 367-375.
Thomas, T. and Dziadek, M. (1993). Capacity to form choroid plexus-like cells in vitro is restricted to specific regions of the mouse neural ectoderm. *Development* **117**, 253-262.
Wallace, V. A. (1999). Purkinje-cell-derived Sonic hedgehog regulates granule neuron precursor cell proliferation in the developing mouse cerebellum. *Curr. Biol.* **9**, 445-448.
Wechsler-Reya, R. J. and Scott, M. P. (1999). Control of neuronal precursor proliferation in the cerebellum by Sonic Hedgehog. *Neuron* **22**, 103-114.